Functional Significance of Cardiac Myosin Essential Light Chain Isoform Switching in Transgenic Mice

Jason G. Fewell,* Timothy E. Hewett,* Atsushi Sanbe,* Raisa Klevitsky,* Eric Hayes,‡ David Warshaw,‡ David Maughan,‡ and Jeffrey Robbins*

**Department of Pediatrics, Division of Molecular Cardiovascular Biology, Children's Hospital Research Foundation, Cincinnati, Ohio 45229-3039; and ‡Department of Molecular Physiology and Biophysics, University of Vermont, Burlington, Vermont 05405-0068*

Abstract

The different functions of the ventricular- and atrial-specific essential myosin light chains are unknown. Using transgenesis, cardiac-specific overexpression of proteins can be accomplished. The transgenic paradigm is more useful than originally expected, in that the mammalian heart rigorously controls sarcomeric protein stoichiometries. In a clinical subpopulation suffering from heart disease caused by congenital malformations of the outflow tract, an ELC1vÆELC1a isoform shift correlated with increases in cross-bridge cycling kinetics as measured in skinned fibers derived from the diseased muscle. We have used transgenesis to replace the ventricular isoform of the essential myosin light chain with the atrial isoform. The ELC1v→ELC1a shift in the ventricle resulted in similar functional alterations. Unloaded velocities as measured by the ability of the myosin to translocate actin filaments in the in vitro motility assay were significantly increased as a result of the isoform substitution. Unloaded shortening velocity was also increased in skinned muscle fibers, and at the whole organ level, both contractility and relaxation were significantly increased. This increase in cardiac function occurred in the absence of a hypertrophic response. Thus, ELC1a expression in the ventricle appears to be advantageous to the heart, resulting in increased cardiac function. (*J. Clin. Invest.* 1998. 101:2630–2639.) Key words: sarcomere • heart • muscle • mouse • hypertrophy

Introduction

In striated muscle, the sarcomeric proteins are usually represented by multiple isoforms. These isoforms result either from transcription of different members of a multigene family, differential splicing patterns of a primary transcript, or a combination of the two processes (1, 2). The particular isoform expressed is dependent upon the muscle type, and can be developmental stage–specific (3). The multiplicity of isoforms probably underlies the different physiologic behaviors of the unique muscle types, although in many cases their functional significance remains obscure.

These points are particularly relevant to the proteins making up the molecular motor of striated muscle: the myosin heavy (MyHC)[1] and light chains. Intact myosin is a hexameric molecule consisting of two heavy chains as well as two regulatory and two essential light chains (4). In the mammalian heart, the two heavy chain genes—α-*MyHC* and β-*MyHC*—have been extensively studied. They are expressed in a developmental stage–specific and compartment-specific manner, and the relative proportion of the two protein isoforms correlates closely with the speed of contraction (5–7). Similarly, there are multiple isoforms of the essential and regulatory myosin light chains. Essential light chain 1a (ELC1a) is ubiquitously expressed in striated muscle during development, but becomes restricted to the adult atrial compartments (1). Essential light chain 1v (ELC1v) is a ventricular-specific light chain that is also expressed in adult slow skeletal muscle (1). A clear functional role for the ELCs has not been described in cardiac muscle, but they appear to be critical for aspects of the motor's function. For example, in *Dictyostelium*, null mutants for ELC show normal myosin ATPase activity, but cytokinesis does not occur (8, 9). Removing the light chains from chicken skeletal muscle myosin reduced the velocity of actin filament movement by 90% in an in vitro motility assay (10), and decreased isometric force production by $> 50\%$ (11).

In humans, congenital heart defects such as tetralogy of Fallot, double outlet right ventricle, and infundibular pulmonary stenosis lead to the expression of ELC1a in the ventricle (12, 13). Similarly, expression of ELC1a in adult human ventricles can occur in response to dilated cardiomyopathy, and may be related to hypertrophy due to mechanical overload (14, 15). The functional significance of this isoform switch is not clear, but may be a direct compensatory mechanism as the heart attempts to maintain normal cardiac function in response to the primary pathology. A recent study examining cross-bridge kinetics using skinned ventricular fibers from humans having congenital heart defects demonstrated a strong correlation between the amount of ELC1a expressed in the ventricles and the maximal shortening velocity and rate of force development (12). These results suggest that altering ELC isoform composition has a direct effect on muscle fiber function. However, it is not clear how these changes in fiber cross-bridge kinetics would alter whole heart function.

Address correspondence to Jeffrey Robbins, Division of Molecular Cardiovascular Biology, Children's Hospital Research Foundation, Cincinnati, OH 45229-3039. Phone: 513-636-8098; FAX: 513-636-3852; E-mail: jeff.robbins@chmcc.org

Received for publication 15 January 1998 and accepted in revised form 30 March 1998.

J. Clin. Invest.
© The American Society for Clinical Investigation, Inc.
0021-9738/98/06/2630/10 $2.00
Volume 101, Number 12, June 1998, 2630–2639
http://www.jci.org

1. *Abbreviations used in this paper:* ELC1a, essential light chain 1a; ELC1v, essential light chain 1v; GAPDH, glyceraldehyde-3-phosphate dehydrogenase; HR, heart rate; mpm, meters per minute; MyHC, myosin heavy chain; NTG, nontransgenic; RT, reverse transcription; TG, transgenic.

Isoform replacement of the cardiac myosin light chains can be accomplished through transgenic overexpression of the protein (16, 17). This approach gives one the ability to study the significance of the isoform switch on cardiac structure and function in a controlled setting without the pleiotropic effects of the disease state with which this isoform switch is normally associated. We were interested in testing the hypothesis that an ELC1v→ELC1a switch in the ventricle leads to an increase of unloaded and loaded motor velocity, and possibly cardiac function. Using a cardiac-specific promoter, we transgenically overexpressed ELC1a in the mouse heart, and effected an almost complete replacement of ELC1v with ELC1a in the ventricle. These data show that the isoform switch causes functional increases at the motor, fiber, and whole organ levels.

Methods

Transgene construction. A full-length murine ELC1a cDNA was synthesized using reverse transcription (RT)-PCR with poly A^+ RNA isolated from atrial tissue of FVB/N mice as template. Primers with SalI sites at the termini were made to the 3′ and 5′ untranslated regions of the ELC1a cDNA (see Fig. 1). The PCR product was sequenced, and the fragment was linked to the mouse α-MyHC promoter (see Fig. 1). The final construct was digested free of vector sequence with NotI, purified from agarose, and used to generate transgenic mice as described (18).

Transcript analysis. Total atrial and ventricular RNA was prepared from freshly isolated tissue obtained from mice killed by CO_2 asphyxiation. Samples were homogenized in Tri-Reagent™ (Molecular Research Center, Inc., Cincinnati, OH), and RNA was extracted according to the manufacturer's protocol. For each analysis, 2 μg of total RNA was loaded onto a nylon membrane (Zeta-probe™; Bio-Rad Laboratories, Hercules, CA) using a dot blotting apparatus (Bio-Rad Laboratories). Hybridizations using ^{32}P–end-labeled oligonucleotides have been described (19). Oligonucleotide sequences that were used as probes (ELC1a, ELC1v, glyceraldehyde-3-phosphate dehydrogenase [GAPDH] α-skeletal actin, atrial natriuretic factor [ANF], and β-MyHC) have been reported (20).

Myofilament protein preparation and SDS-PAGE gel electrophoresis. For SDS-PAGE, the left ventricular apex and atrial flaps were obtained from killed ELC1a transgenic (TG) and nontransgenic (NTG) mice. Samples enriched for the myofibrillar proteins were obtained as described previously (21). Gel preparations, electrophoretic conditions, and gel staining have been described (22).

Immunofluorescent analysis and confocal microscopy. For immunofluorescent detection of ELC1a, mice were anesthetized with isofluorane, and the hearts were fixed by perfusion with 4% paraformaldehyde in PBS. The hearts were then removed and further fixed in 4% paraformaldehyde in PBS for 2 h at 4°C. After fixation, the hearts were sucrose-infiltrated in a solution containing 30% sucrose in PBS overnight at 4°C, and were then embedded in O.C.T. compound (Miles Laboratories, Inc., Elkhart, IN). Sections (5 or 7 μm) were incubated with rabbit polyclonal antisera against ELC1a (Genemed Biotechnologies, Inc., San Francisco, CA), and with a monoclonal antibody against α-actinin (Sigma Chemical Co., St. Louis, MO). The epitope used to generate the ELC1a antibody was a 13–amino acid sequence (LKDSAFDPKSVKI) corresponding to amino acids 30–42 of ELC1a (see Fig. 1 *B*). Secondary antibodies used were either conjugated to FITC (ELC1a) or Texas Red (α-actinin). Double-labeled sections were visualized using confocal microscopy (Molecular Dynamics, Inc., Sunnyvale, CA) driven by a Silicon Graphics workstation.

Actin motility assay. Myosin used for the in vitro motility assay was extracted from ventricular tissue samples that had been frozen in liquid nitrogen. The methods describing the myosin extraction procedure from 10-mg samples and conditions for measuring actin filament velocity in the motility assay have been described elsewhere (23).

Measurements of fiber function. Standard methods for measuring force development from skinned muscle fibers were adapted for mouse cardiac fibers as follows. Mice were injected with heparin (500 IU/kg intraperitonally) 5 min before being killed. To prepare skinned fibers, the heart was removed and placed in a relaxing solution (5.37 mM ATP, 30 mM phosphocreatine, 5.0 mM EGTA, 20 mM BES, 7.33 mM $MgCl_2$, 0.12 mM $CaCl_2$, 10 mM DTE, 10μg/ml leupeptin, and 32 mM potassium methansulfonate, pH 7.0) at 4°C. The relaxing solution also contained 30 mM 2,3-butanedione monoxime designed to protect myocardial tissue from cutting injury (24). Small sections of left ventricular papillary muscles were dissected, yielding muscle fibers of an ~ 0.5-mm diameter and a 2–3-mm length. The fiber strips were skinned by incubation in 5.5 mM ATP, 5.0 mM EGTA, 20 mM BES, 6.13 mM $MgCl_2$, 0.11 mM $CaCl_2$, 10 mM DTE, 10 μg/ml leupeptin, 121.8 mM potassium methansulfonate, pH 7.0, and 50% glycerol with 0.5% (wt/vol) Triton X-100 for 12 h at 4°C. The fiber strips were then transferred to fresh solution without Triton X-100, and were stored at −20°C until used. All skinned fiber experiments were performed using a commercially available apparatus (Scientific Instruments, Heidelberg, Germany). Dissected fibers (150–200-μm diameter and 1.3–2.0-mm length) were mounted isometrically between a force transducer and a length-step generator in relaxing solution. Sarcomere length (determined by laser diffraction analysis) at resting tension was always 2.0–2.1 μm. Contraction solution had the same composition as the relaxing solution, except that EGTA was substituted with 5 mM [Ca^{2+}]EGTA. Free Ca^{2+} concentration was obtained by mixing relaxation and contraction solutions in the appropriate proportions. Strip tension (mN/mm^2) was calculated by dividing force by fiber cross-sectional area, calculated from widths measured at the major axis. V_{max} was obtained by the slack test using a method modified from one described elsewhere (25, 26). In brief, release amplitudes were introduced to one end of the fiber that varied within 7–14% of initial muscle length. Release abolished tension completely. After the onset of tension recovery, the fiber was restretched to the initial muscle length. Slack time was defined as the time between completion of the length step and the moment at which force began to redevelop.

Ex vivo whole heart measurement and telemetry. The Langendorff (27) and working heart (20) preparations were performed as described previously with the modifications described by Gulick et al. (17). Surgical implantation of EA-F20 telemetry devices (Data Sciences International., St. Paul, MN) were performed according to the manufacturer's instructions, and in accordance with the *Guide for the Care and Use of Laboratory Animals*. Resting and maximal heart rates (HR) were obtained after a previously described protocol with modifications (22). Specifically, to determine maximal HR, the animals were submitted to an exercise regimen using a four-lane treadmill (OmniPacer LC4™; Omnitech Elec., Inc., Columbus, OH). The animals were placed in the treadmill and allowed to acclimate for 5 min. The animals then ran at 10 m per min (mpm) for 15 min, and heart rate was determined. Speed was incrementally increased (20, 23, 25 and 27 mpm) over 3-min intervals. HRs were determined after 2 min at each speed.

Results

A cDNA encoding ELC1a was produced (Fig. 1 *A*) using RT-PCR as described in Methods. Multiple clones were sequenced in order to exclude any PCR-induced errors. A consensus sequence identical to that previously reported for mouse ELC1a (28) was obtained. The lack of conservation between the compartment-specific isoforms is striking (Fig. 1 *B*). In particular, the amino halves of the proteins are highly divergent, and this portion of the protein may well have a functional interaction with actin (see Discussion). The cDNA was placed into the α-MyHC promoter cassette, which contains the full-length

A

```
GTCGACGAGC CTAAAGCAAC ATGCCTCCCA AGAAACCCGA GCCTAAGAAG GAGACTGCCA AGCCGGCTGC
AGCCCCTGCT CCAGCTGCAT CCGCAGCTCC GGAGCCCCTC AAGGACTCTG CCTTTGACCC AAAGAGTGTG
AAGATAGACT TCAGTGCTGA CCAGATCGAA GAATTCAAAG AGGCCTTTTC ATTGTTTGAC CGGACTCCAA
CGGGAGAGAT GAAGATCACC TACGGGCAGT GTGGGGACGT GCTGCGGGCC CTGGGCCAGA ACCCCACCAA
CGCAGAGGTG CTGCGCGTTT TGGGCAAACC CAAGCCTGAA GAGATGAGTT CCAAGACACT GGACTTCGAG
ATGTTCCTGC CCATCCTGCA ACACATCTCC CGCAACAAGG AGCAGGGCAC CTATGAGGAC TTCGTGGAGG
GGCTGCGGGT CTTTGACAAA GAAAGCAACG GCACAGTCAT GGGTGCCGAG CTTCGGCATG TCCTTGCCAC
CCTGGGAGAG AAGATGAGCG AGGCAGAGGT GGAGCAGCTG TTGTCTGGGC AGGAGGATGC CAATGGCTGC
ATCAACTATG AAGCCTTTGT CAAGCACATC ATGTCTGGGT AAAGCACGTT TCTCCAGGGT GGTCGAC
```

B

```
ELC1a  MPPKKPEPKKETAKPA---AAPAPAASAAPEPLKDSAFDPKSVKIDFSAD--------QIEEFKE
       • ••••••••  •• •   •••••••  •  •                      •••••••
ELC1v  MAPKKPEPKKDDAKAAAPKAAPAPAAAPAAAPAAAPEPERPKEAEFDASKIKIEFTPEQIEEFKE

ELC1a  AFSLFDRTPTGEMKITYGQCGDVLRALGQNPTNAEVLRVLGKPKPEEMSSKTLDFEMFLPILQHI
       •• •••••• •••••••••••••••••••••• •••••••••• ••  ••  ••• ••• ••••
ELC1v  AFLLFDRTPKGEMKITYGQCGDVLRALGQNTPQAEVLRVLGKPKQEELNSKMMDFETFLPMLQHI

ELC1a  SRNKEQGTYEDFVEGLRVFDKESNGTVMGAELRHVLATLGEKMSEAEVEQLLSGQEDANGCINYE
       • ••  ••••••••••••••• ••••••••••••••••••   • ••• •  •••• •••••••
ELC1v  SKNKDTGTYEDFVEGLRVFDKEGNGTVMGAELRHVLATLGERLTDEEVEKLMAGQEDSNGCINTE

ELC1a  AFVKHIMSG
       •••••••
ELC1v  AFVKHIMAS
```

C

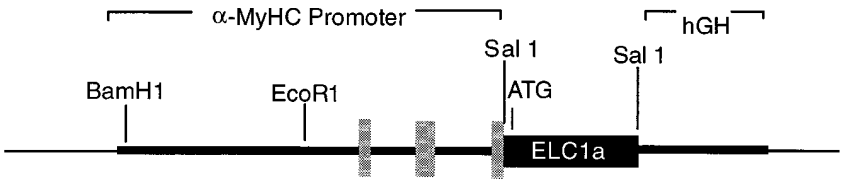

Figure 1. ELC isoforms and construct used for the generating transgenic mice. (*A*) Nucleotide sequence of ELC1a used to make the transgenic construct. The start and stop codons are in bold type. The underlined sequences correspond to the parts of the 5′ and 3′ untranslated regions that were included in the primers for the RT-PCR; these also contained engineered SalI restriction sites (*italics*) at the extreme flanking ends, which were used to clone the cDNA into the α-MyHC promoter. (*B*) Amino acid comparison of the ventricular and atrial essential light chains. Note the significant variability between the two isoforms at the amino termini. (*C*) Schematic representation of the construct used to generate transgenic animals. ELC1a is linked to the 5.5-kb α-MyHC promoter containing the first three noncoding exons (*grey boxes*) of the α-MyHC transcript. Immediately after the ELC1a sequence is a portion (~ 600 bp) of the human growth hormone (*hGH*) gene containing a polyadenylation signal.

α-MyHC transcriptional apparatus upstream, and a human growth hormone polyadenylation signal downstream of the cDNA's insertion site (Fig. 1 *C*). Five transgenic founder lines carrying varying numbers of the transgene (Fig. 2 *A*) were used to establish stable lines by outbreeding to NTG animals. RNA blot analyses were carried out on these offspring to determine the amount of TG transcript being produced. (Fig. 2 *A*). As expected on the basis of previous lines generated with this promoter construct, expression levels differed between the lines, varying from barely over background levels (line 46; 1.3-fold) to robust overexpression (line 34; 13-fold increase as compared with ELC1a levels expressed in the NTG atria). The other three lines (57, 80, and 67) had intermediate expression levels of 6.0-, 5.5-, and 1.8- fold increases over control levels, respectively (Fig. 2 *A*).

The sarcomere's capacity for maintaining protein stoichiometry within the contractile apparatus, even when transcript expression levels are increased 5–30-fold via transgenic manipulation, is a phenomenon observed previously when the ventricular and skeletal regulatory light chains were overexpressed in the heart (16, 17). Thus, the degree of replacement is a function of the level of overexpression, as well as the ectopic protein's affinity for the compartment's contractile apparatus (17). Incorporation of the ectopically expressed ELC1a in the ventricles of TG mice was determined by both SDS-PAGE electrophoresis and by immunofluorescent analysis. The species present in the myofilaments were separated on 16% SDS-polyacrylamide gels; the data show significant ELC1a protein levels in the ventricles of all but one of the founder lines (Fig. 2 *B*). No shifts in the other major protein

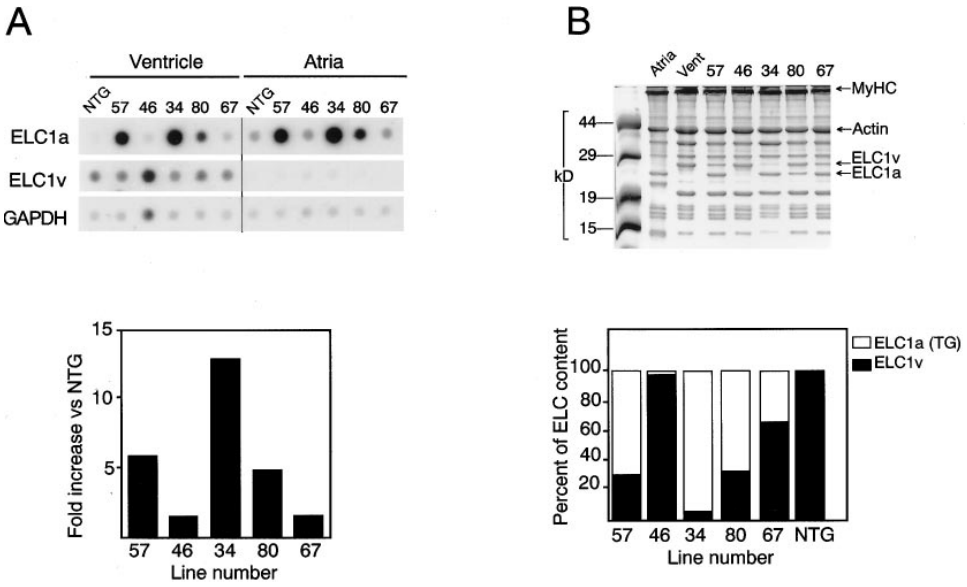

Figure 2. Analysis of ELC1a RNA and protein expression. (*A*) Five ELC1a TG lines were analyzed and compared with NTG controls. For each analysis, 2.5 μg of total RNA obtained from atrial and ventricular tissue was loaded onto a nylon membrane. Hybridization was performed using transcript-specific ^{32}P-labeled oligonucleotides as indicated. Hybridization signals were quantitated using a PhosphoImager (Molecular Dynamics, Sunnyvale, CA), and relative levels between different RNA samples were normalized to GAPDH expression levels (*bottom*). Note that even when ventricular RNA from line 46 is overloaded, transgene expression is barely detectable. There were no significant differences in expression levels between animals from the same line (data not shown). The DNA copy number for each of the transgenic lines (determined by Southern blot analysis) is as follows: line 57, 7 copies; line 46, 3 copies; line 34, 8 copies; line 80, 6 copies; line 67, 2 copies. (*B*) Analysis of myofibrillar protein composition of ventricular tissue. A total of 7.5 μg of TG myofilament ventricular protein was loaded onto each lane of a 16% SDS polyacrylamide gel, and was electrophoresed for 2 h at 25 mA. The five ELC1a TG lines show different amounts of ELC1a being ectopically expressed in the ventricles. Atria, NTG myofilament protein derived from atria; Vent, NTG myofilament ventricular protein. Protein levels were determined by densitometry, and relative amounts of ELC1a and ELC1v protein are presented in the lower panel as a percent of the total ELC content, which was invariant.

isoforms of the contractile apparatus (MyHC, actin, regulatory light chains) could be detected (data not shown). Quantitation of ELC content revealed a > 95% replacement of ELC1v with ELC1a in line 34, with less replacement in lines 46, 57, 67, and 80. With the exception of line 67, the amount of protein replacement correlated well with the amount of ELC1a transcript being expressed. As expected, the gels show that TG overexpression of ELC1a does not lead to a net increase in the amount of ELC, but rather, as ELC1a protein levels increase, ELC1v protein decreases proportionately.

Although the data in Fig. 2 *B* suggest that protein is being incorporated into the myofibril, we were interested in looking at sarcomeric organization more directly. To this end, frozen sections obtained from line 34 mice were examined by immunofluorescent detection using an antibody raised against the ELC1a-specific peptide LKDSAFDPKSVKI (Fig. 3). Low magnification of sections labeled with ELC1a antibody conjugated to FITC shows high levels of labeling in the atria of NTG animals, and no detectable signal in the ventricles. In contrast, both the atria and ventricles derived from TG animals are labeled with the ELC1a antibody (Fig. 3 *A*). Sections were then double-labeled with α-actinin, which binds at the Z-bands and with ELC1a. Confocal microscopy shows that in atria, α-actinin labeling is tight and regularly spaced (Fig. 3 *B*). ELC1a labeling in NTG atria shows a regular striated pattern that is consistent with labeling of the portion of the sarcomere containing myosin (Fig. 3 *B*). When the α-actinin- and ELC1a-labeling patterns are overlaid, it is clear that they are distinct from one another, a staining pattern that is consistent with the spatial organizational patterns of the two proteins in the sarcomere. In NTG ventricles, distinct α-actinin labeling is apparent, but no ELC1a labeling can be seen (Fig. 3 *C*). In TG ventricles, the ELC1a labeling shows a striated pattern similar to that observed in NTG atria (Fig. 3 *D*).

In some cases, ELC1a is expressed in ventricular tissue in response to hypertrophy. Although ELC1a expression is almost certainly a secondary response, this has not been rigorously tested. Thus, we were interested in determining if transgenic expression of ELC1a in the ventricles of mice led to a significant hypertrophic response. At the molecular level, increases in transcript expression levels of β-MyHC, α-skeletal actin, and ANF are associated with hypertrophy (29–32). When the levels of these transcripts were examined in ventricles derived from mice showing high levels of ELC1a replacement (lines 34 and 57), no increases could be detected (Fig. 4). Consistent with these data, no increases in compartment mass normalized to body weight were observed (Table I). These data show that a detectable cardiac hypertrophic response does not occur in the TG mice.

In fibers derived from patients with congenital heart defects, ELC isoform switching is correlated with increases in V_{max} of shortening velocity and rate of force development (12). This result suggests that differences in ELC isoforms can somehow lead to a modulation of the contractile properties of the molecular motor. To determine if functional alterations are associated with overexpression of ELC1a in the ventricles, TG myosin was analyzed for its ability to move actin in an vitro motility assay (Fig. 5). The results from these experiments show that myosin from the ventricles of the TG mice translocated actin at a significantly higher rate than that of myosin from NTG ventricles and demonstrate that alterations in the ELC isoform composition have a direct impact on unloaded motor velocity.

There are significant changes in the contractile properties of

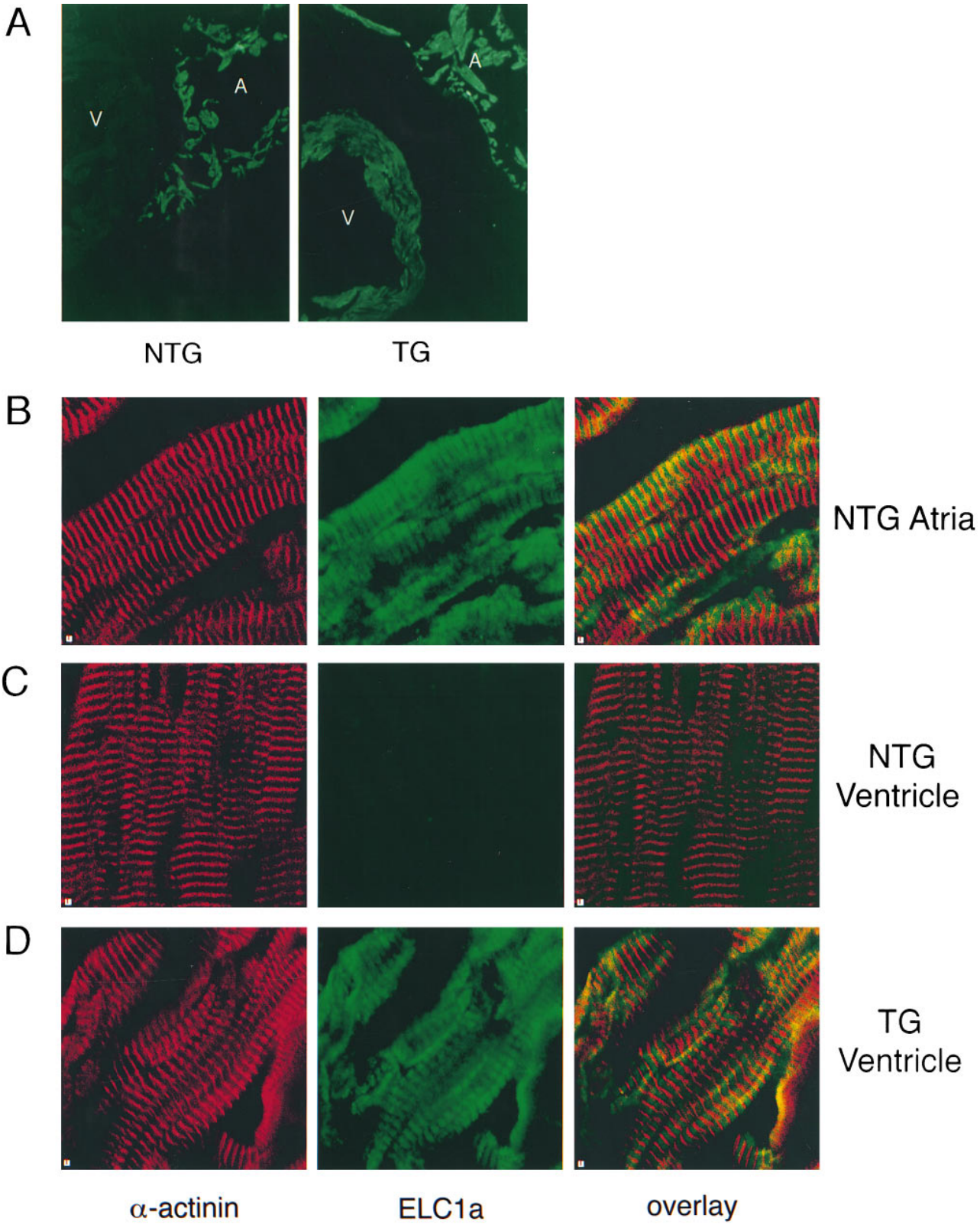

Figure 3. Immunofluorescent analysis of ELC1a expression in the ventricles and atria of ELC1a TG and NTG mice. (*A*) Low magnification of atrial and ventricular tissue from line 34 mice showing expression of ELC1a in TG ventricles and the absence of expression in NTG controls (40×). (*B–D)* High magnification (600×) confocal images of the sarcomeric structure of atrial and ventricular NTG and TG tissue labeled with α-actinin (Texas red) and ELC1a (FITC). All images were obtained under identical settings, and therefore comparisons among different tissues could be made. (*B*) Atrial tissue from an NTG heart. The third panel is an overlay of the first two panels. The yellow color indicates areas where expression of both α-actinin and ELC1a occur. (*C*) Ventricular tissue from an NTG heart fluorescently labeled as in Fig. 3 *B*. No ELC1a can be detected (*middle*). (*D*) Ventricular tissue from an ELC1a TG heart labeled with antibodies as in *B* and *C*. Note the high levels of ELC1a labeling compared with the NTG ventricle and the lack of ELC1a in the α-actinin staining Z bands.

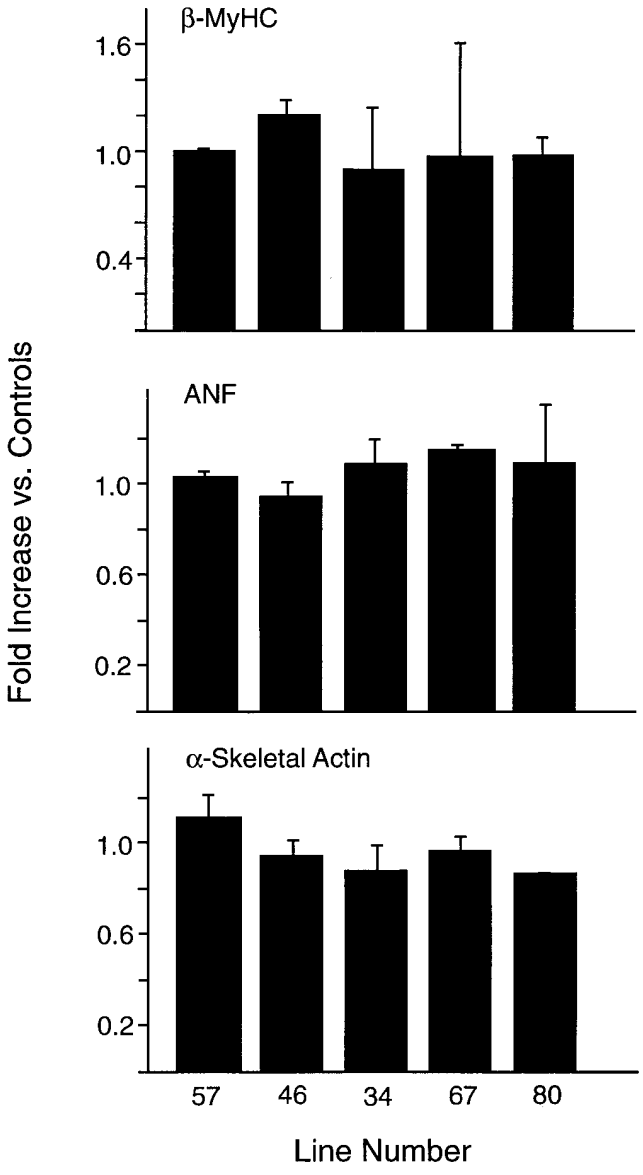

Figure 4. Transcript expression of molecular markers of hypertrophy. Transcript levels of atrial natriuretic factor, α-skeletal actin, and β-MyHC were quantitated in the five TG lines using transcript-specific oligonucleotide probes, and were normalized to GAPDH expression levels. In all cases ($n = 3$), no significant differences were noted when compared with NTG controls.

skinned fibers obtained from human ventricles exhibiting ELC isoform switching. Specifically, an increase in the V_{max} of shortening correlates with increasing amounts of ELC1a expression (12). We were interested in determining if cardiac fiber mechanics were affected by ELC isoform switching in the TG model. Skinned fibers were prepared from left ventricular papillary muscle, and the velocity of unloaded shortening was measured using the slack test (Fig. 6). The maximum force developed was not altered in the TG mice compared with the NTG controls (TG, 9.90±0.68 mN/mm^2; NTG, 9.47±0.63 mN/mm^2). However, a significant (1.78-fold) increase in V_{max} of TG fibers as compared with NTG controls was observed (Fig. 6, *B* and *C*).

Table I. Heart Chamber Weights from TG and NTG Animals

	n	HW/BW	A/BW	LV/BW	RV/BW
		mg/g	*mg/g*	*mg/g*	*mg/g*
Line 37	6	4.21±0.05	0.21±0.01	3.40±0.07	0.57±0.03
Line 57	8	4.28±0.12	0.21±0.02	3.35±0.08	0.70±0.04
NTG	16	4.10±0.06	0.25±0.01	3.24±0.05	0.61±0.03

Values are means±SE. HW, heart weight; BW, whole body weight; A, summed atrial weight; LV, left ventricular weight; RV, right ventricular weight.

A logical extension of these studies was to determine if the changes at the motor and fiber levels translate into changes in contractile function at the whole heart level. Using the isolated perfused hanging heart, ventricular contractile function was determined (Table II). Line 34, which has > 95% replacement, and line 57, which has 68% ELC1a protein replacement in the ventricles (Fig. 2 *B*), were both studied in an attempt to establish a dose response. In both the working and Langendorff heart preparations, the TG hearts are hypercontractile as compared with controls. Specifically, ±dP/dt are increased. This result is particularly striking in the Langendorff heart preparation, where the magnitude of the change is sufficient such that a dose response becomes apparent: as the degree of replacement increases, the hypercontractile response becomes greater. These data are also consistent with the working heart where, in line 34, there is a 10% increase in +dP/dt, while no increase is detected in line 57. The mean relaxation rates (−dP/dt) were increased in both lines 34 and 57 under working heart conditions. However, only line 57 demonstrated a significant (11%) increase.

In both of the working heart preparations, the unpaced HRs were significantly lower in both line 34 and 57 animals when compared with controls, and the magnitude of the decrease appeared to be dose-dependent. To determine if these changes were physiologically relevant, the in vivo HRs in unrestrained TG and NTG mice were determined. Measurements of resting HRs as well as HRs at increasing exercise intensity

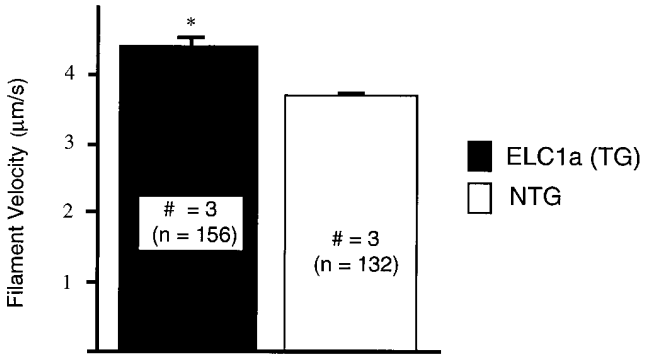

Figure 5. In vitro motility assay of ELC1a TG (line 34) and control mice. This bar graph indicates the velocities of actin filaments (micrometers per second) of ELC1a TG and NTG animals. Values are expressed as means±SEM. #, number of mice; n, number of actin filaments analyzed. *$P < 0.0001$.

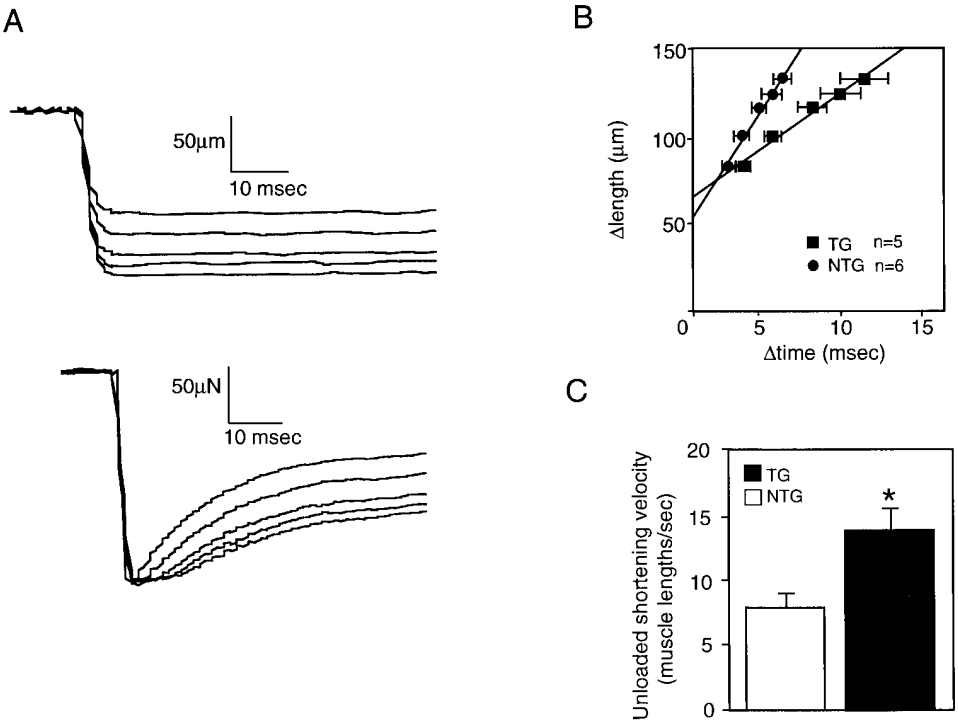

Figure 6. Contractile properties of isolated ventricular fibers. *(A)* Shown are a typical set of tracings derived from ventricular skinned fibers subjected to the slack test at $pCa^{2+} = 5.0$. The changes in force (*bottom*) in response to five different amplitudes of length release (7.8, 9.3, 10.7, 11.6, and 12.5%,; *top*) are shown. *(B)* Slack test comparison between TG (line 34) and NTG mice. The change in length (*Δ length*) was plotted vs. the time lag between the onset of a release and the onset of tension recovery (*Δ time*). Straight lines were then fitted by the least-squared method. (*C*) Mean V_{max} of TG and NTG mice. The slope of the regression (*A*) provided the measure of V_{max}. Values are expressed as means± SEM. $*P < 0.05$.

were determined using an implantable telemetry device in a lead II configuration as previously described (22). The resting HR of TG mice, obtained when the mice were sleeping in their cages, show no significant differences when compared with NTG littermates (Fig. 7), although there was a trend towards a slower basal HR for the TG animals. In response to treadmill exercise, the HR of TG animals is significantly lower than that of NTG animals at the lowest exercise intensity (10 mpm). However, at higher speeds there are no significant differences between TG and NTG animals, although mean HR of TG animals is consistently lower than NTG controls at all exercise intensities. It is interesting to note that the NTG heart rate appears to be at or near maximum values at all treadmill speeds, while the HR of TG animals is initially much lower than NTG HR, but increases in response to an increase in treadmill speed.

Discussion

The data show that transgenesis can be used to direct an essential light chain isoform switch in the murine heart, successfully mimicking a phenomenon that can accompany various human congenital heart malformations and dilated cardiomyopathy. Transgenic overexpression of ELC1a using the α-MyHC promoter leads to high levels of transcript expression in both atria and ventricles. However, the protein content of the atria is unaffected, while in the ventricles, ectopically expressed ELC1a replaces the endogenously expressed ELC1v with no net increase in ELC content. These data demonstrate the tremendous capacity the myocyte has for maintaining sarcomeric stoichiometry, and are consistent with previous results in which the different myosin light chains were overexpressed in TG mice (16, 17). The mechanistic basis of this regulation is not

Table II. Means±SEM of Measured Cardiac Parameters

	Control	ELC1a (34)	% Change	Control	ELC1a (57)	% Change
Working Heart	76 ($n = 8$)	70 ($n = 8$)		75 ($n = 10$)	70 ($n = 7$)	
heart rate (beats per minute)	376±6	334±6	−11***	366±4	342±3	−7*
+dP/dt (mmHg/s)	5976±178	6549±188	+10*	5818±159	5868±137	0
−dP/dt (mmHg/s)	4183±77	4392±91	+5	4140±84	4593±78	+11§
Langendorff Heart	78 ($n = 8$)	80 ($n = 8$)		100 ($n = 10$)	80 ($n = 8$)	
heart rate (beats per min)	313±6	329±5	+5*	340±6	308±10	−9‡
+dP/dt (mmHg/s)	1582±76	2357±70	+49§	2296±55	2471±62	+8*
−dP/dt (mmHg/s)	979±41	1374±40	+40§	1566±46	1763±56	+13‡

$*P \leq 0.05$, $‡P \leq 0.01$, $§P \leq 0.001$, ELC1a transgenic vs. control, unpaired Student's *t* test.

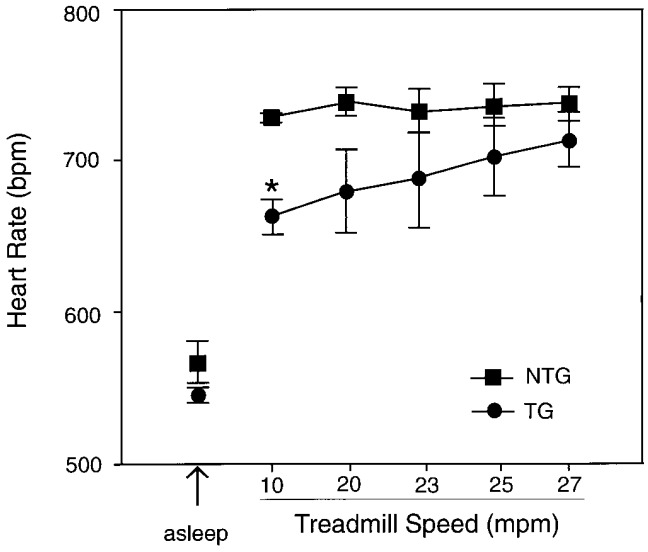

Figure 7. Measurement of resting and active HRs using implantable telemetry devices. Basal HR of TG (line 34) and NTG mice were acquired while the animals were sleeping in their cages. The line graph shows a comparison between TG and NTG response to increasing exercise: 10, 20, 23,25, and 27 mpm at a 7° incline. Values are expressed as means±SEM. $*P < 0.05$.

clear, but preliminary data indicate that it occurs at the post-transcriptional level since we are unable to detect any alterations in the steady-state level of the relevant, endogenous mRNAs (Robbins, unpublished observations).

ELC1a replacement in the ventricles does not lead to development of hypertrophy. In humans, in addition to the expression patterns observed with the congenital abnormalities, ELC1a expression in the ventricles is associated with hypertrophy resulting from mechanical overload (15). Interestingly, in end-stage heart failure, the appearance of ELC1a in the ventricles is not detected (33). Thus, the accepted interpretation is that ELC1a expression in the ventricles is a compensatory mechanism that is lost in late- stage heart failure during decompensation. The data obtained from the ELC1a TG mice show that the isoform transition can lead to significant alterations in both motor and heart function in the absence of significant hypertrophy. Histological examination of hearts obtained from young to middle-aged adults (5–24 wk) revealed no overt pathology or fibrosis at any developmental stage (data not shown). We conclude that the isoform switch is a secondary compensatory response designed to maintain cardiac function in the face of other primary lesions.

Replacing ELC1v with ELC1a has a clear effect on molecular motor function. The isoform switch results in a significant increase in the sliding velocity of myosin in an actin motility assay. An examination of the primary structures of ELC1a and ELC1v underlies the possible mechanistic basis of this functional change. Much of the heterogeneity between the two proteins occurs at the amino terminal end within the tether region of the ELCs (Fig. 1). This portion of the molecule interacts with actin, and can modulate contractile function by inhibiting the rate at which myosin cycles (34, 35). When the interaction between ELC and actin is ablated, the rate of fiber shortening is increased (36). Similarly, other in vitro studies show that replacement of an ELC containing a tether with the fast skeletal isoform (which lacks the tether) leads to a similar alteration of function (34). Considering the lack of conservation in the ELC1a and ELC1v proteins in this critical region, it is reasonable to propose that the two proteins have different actin interactive properties; changes in these interactions as a result of isoform switching might lead to the functional alterations detected in this study. It is possible that the length differences between the light chains in this region (ELC1a being shorter that ELC1v) modulates myosin cycling rates. As ELC1a is shorter than ELC1v, the amount of interaction between the ELC and actin may be reduced, effectively attenuating the tether action and leading to increased function. We are currently testing this hypothesis directly by preparing mice in which the tether lengths are modified.

Alternatively, the observed alteration may occur through a more indirect pathway. Whittaker et al. (37) showed that the light-chain binding domain on the MyHC is at a pivotal area within the hinge region of the myosin head. They proposed that small changes in the myosin ATP-binding cleft during hydrolysis could be transduced to the light-chain binding domain where relatively small movements of the head are amplified into large movements of the hinge and lever arm, leading to the full range of myosin movement during contraction. Thus, it is plausible that by altering the ELC isoform content, one could influence movement in this critical region of myosin, leading to the observed changes in sliding velocities.

As a result of the isoform switch, there are significant alterations in both unloaded and loaded function as measured by the in vitro motility assay and whole heart mechanics, respectively. An examination of skinned fiber function, as measured by the slack test, indicates that the fibers from TG mice have a higher V_{max} of shortening when compared with NTG controls. Significant increases in the measured velocities for both the slack test (1.78-fold) and in vitro motility assay (1.17-fold) occurred as a result of the isoform switch. The magnitude of these changes differed between the different assays, although both are normally thought to be measurements of unloaded shortening velocities. However, the skinned fiber is a complex system in which the contractile machinery operates against an internal cytostructure in both the sarcomere and connective tissue. Therefore, V_{max} in a fiber is never truly unloaded as it is assumed to be in the motility assay, and the fiber estimates are complicated by the motor working along its force/velocity relationship. Thus, it is not surprising that the quantitative measurements differ in their magnitudes. Fibers obtained from diseased human hearts similarly show a positive correlation between V_{max} of shortening and ELC1a replacement in the ventricles. In the human heart, a 20% replacement of ELC1v with ELC1a was accompanied by a 1.88-fold increase in V_{max} of shortening (12). However, in the mouse, an $\sim$ 95% replacement leads to a 1.78-fold increase in V_{max}. Although the data are consistent, it appears that the effect in the mouse is attenuated as compared with the human. Similarly, Morano's group noted a correlation between the appearance of ELC1a in the ventricle and an increase in the Ca^{2+} sensitivity of the fiber (38). We also noted a small shift to the left in the force–Ca^{2+} curve derived from the TG fibers, although it did not reach statistical significance (data not shown). Perhaps the differences in the magnitude of the effect are due to inherent differences in the cardiac cycle between humans and small rodents, and also to the fact that it is not physically possible to enhance

shortening velocities any further in the mouse heart, which, at maximum cardiac stress, beats at approximately 1.5 times that of the resting heart rate in the sleeping animal (Fig. 7). Alternatively, the data derived from the human samples may also reflect unanticipated changes in the other sarcomeric proteins. For example, recent data indicate that significant amounts of α-*MyHC*–encoded protein are present in the human ventricle (39, 40), and failure is accompanied by downregulation of this species with a concomitant upregulation of β-*MyHC*–encoded transcript. This isoform shift could also explain the increases observed by Morano et al. (12, 38).

Importantly, ELC switching in the ventricles of the mouse heart leads to hypercontractile function at the whole heart level. Parameters of both relaxation ($-dP/dt$) and contraction ($+dP/dt$) are significantly increased in the Langendorff preparations, and in a transgene dose-dependent fashion. The alterations in whole heart function are consistent with the changes occurring at the molecular level of the motor, as myosin from TG mice translocates actin at significantly higher rates than those observed in control preparations, and are also consistent with the increases observed in the unloaded shortening velocity of the TG skinned fibers. These changes in cardiac function appear to have functional consequences at the whole animal level as well. The mean HR of TG mice is consistently lower then that of NTG controls, although in many cases the differences do not reach statistical significance. In response to an exercise regimen, the HR of TG mice is significantly lower at the lowest exercise intensity, but not at the high levels due to the increase in HR of TG mice. The HR of NTG animals remains relatively unchanged throughout the exercise regimen. Thus, it is possible that in the TG animals, enhancement of cardiac function leads to greater stroke volumes and a lowering of HR in order to maintain cardiac output. This effect is most apparent in response to the exercise regimen where NTG animals are at or near maximal levels, even at the lowest intensity level. In contrast, TG mean HR values continue to increase throughout the exercise regimen. Presently, it is unclear if the alterations arise from increases in end-diastolic ventricular volume, greater ejection fractions, or both. Experiments are currently in progress to measure both of these parameters using echocardiography on anesthetized mice over the animals' lifetimes as they undergo varying exercise regimens.

To date, we have been unable to detect any pathology resulting from the isoform switch. It may be that the ELC1v→ELC1a isoform switch is completely benign, yet leads to improved cardiac function over the animals' lifetimes. If this is the case, then such an isoform switch may become a target for a treatment modality. It will be interesting to breed these mice with other genetically altered mice in which ventricular function is compromised (41, 42). Perhaps by increasing the amount of ELC1a in the ventricles, development of a dilated cardiomyopathy or hypertrophy due to other defined genetic alterations, and leading to decompensated heart failure, can be attenuated.

In many instances disease states are complex, involving a host of physiological changes that are primary or secondary to the disease. We have shown using transgenesis that it is possible to model in the mouse one consequence of a human disease condition, allowing for rigorous examination of the functional results of one particular aspect of the disease. By taking this approach, it will be possible to dissect various components of different cardiac diseases, and to begin to understand the compensatory mechanisms that contribute to overall cardiac enhancement, or participate in the pathologic functions that eventually result in decompensated heart failure.

Acknowledgments

We thank Lisa Murray for her technical assistance and animal husbandry, and Christine Wolf for technical help.

This work was supported by National Institutes of Health grants HL56370, HL41496, HL52318, and HL56620, by the Marion Merrell-Dow foundation (to J. Robbins), and by an American Physiological Society postdoctoral fellowship in mammalian organ system physiology to J. Fewell.

References

1. Barton, P.J.R., A. Cohen, B. Robert, M.Y. Fisman, F. Bohhomme, J. Guenet, D.P. Leader, and M. Buckingham. 1985. The myosin alkali light chains of mouse ventricular and slow skeletal muscle are indistinguishable and encoded by the same gene. *J. Biol. Chem.* 260:8578–8584.

2. Buckingham, M.E. 1989. The control of muscle gene expression: a review of molecular studies on the production and processing of primary transcripts. *Brit. Med. Bull.* 45:608–629.

3. Lyons, G.E., S. Schiaffino, D. Sassoon, P. Barton, and M. Buckingham. 1990. Developmental regulation of myosin gene expression in mouse cardiac muscle. *J. Cell Biol.* 111:2427–2436.

4. Schiaffino, S., and C. Reggiani. 1996. Molecular diversity of myofibrillar proteins: gene regulation and functional significance. *Physiol. Rev.* 76:371–423.

5. Barany, M. 1967. ATPase activity of myosin correlated with speed of muscle shortening. *J. Gen. Physiol.* 50:197–216.

6. Whalen, R.G., S.M. Sell, G.S. Butler-Browne, K. Schwartz, P. Bouveret, and I. Pinset-Harstrom. 1981. Three myosin heavy-chain isozymes appear sequentially in rat muscle development. *Nature.* 292:805–809.

7. Schwartz, K., Y. Lecarpentier, J.L. Martin, A.M. Lompre, J.J. Mercadier, and B. Swynghedauw. 1981. Myosin isoenzymic distribution correlates with speed of myocardial contraction. *J. Mol. Cell. Cardiol.* 13:1071–1075.

8. Ho, G., T.L. Chen, and R.L. Chisholm, 1995. Both the amino and carboxyl termini of dictyostelium myosin essential light chain are required for binding to myosin heavy chain. *J. Biol. Chem.* 270:27977–27981.

9. Chisholm, R.L., P. Chen, T.L. Chen, G. Ho, and B.D. Ostrow. 1995. The contributions of light chains to myosin function. *Biophys. J.* 68(Suppl.):223.

10. Lowey, S., G.S. Waller, and K.M. Trybus. 1993. Skeletal muscle myosin light chains are essential for physiological speeds of shortening. *Nature.* 365: 454–456.

11. VanBuren, P., G.S. Waller, D.E. Harris, K.M. Trybus, D.M. Warshaw, and S. Lowey. 1994. The essential light chain is required for full force production by skeletal muscle myosin. *Proc. Natl. Acad. Sci. USA.* 91:12403–12407.

12. Morano, M., U. Zacharzowski, M. Maier, P.E. Lange, V. Alexi-Meskishvili, H. Haase, and I. Morano. 1996. Regulation of human heart contractility by essential myosin light chain isoforms. *J. Clin. Invest.* 98:467–473.

13. Auckland, L.M., S.J. Lambert, and P. Cummins. 1986. Cardiac myosin light and heavy chain isotypes in tetralogy of Fallot. *Cardiovas. Res.* 20:828–836.

14. Schaub, M.C., C.R. Tuchschmid, T. Srihari, and H.O. Hirzel. 1984. Myosin isoenzymes in human hypertrophic hearts. Shift in atrial myosin heavy chains and in ventricular myosin light chains. *Eur. Heart J.* 5:85–93.

15. Schaub, M.C., and H.O. Hirzel. 1987. Atrial and ventricular isomyosin composition in patients with different forms of cardiac hypertrophy. *Basic Res. Cardiol.* 82(Suppl. 2):357–367.

16. Palermo, J., J. Gulick, W.A. Ng, I.L. Grupp, G. Grupp, and J. Robbins. 1995. Remodeling the mammalian heart using transgenesis. *Cell. Mol. Biol. Res.* 41:501–509.

17. Gulick, J., T.E. Hewett, R. Klevitsky, S.H. Buck, R.L. Moss, and J. Robbins. 1997. Transgenic remodeling of the regulatory myosin light chains in the mammalian heart. *Circ. Res.* 80:655–664.

18. Palermo, J., J. Gulick, M. Colbert, J. Fewell, and J. Robbins. 1996. Transgenic remodeling of the mammalian heart. *Circ. Res.* 78:504–509.

19. Robbins, J., J.J. Palermo, and H. Rindt. 1995. In vivo definition of a cardiac specific promoter and its potential utility in remodeling the heart. *Ann. NY. Acad. Sci.* 752:492–505.

20. Jones, W.K., I.L. Grupp, T. Doetschman, G. Grupp, T. Hewett, G. Boivin, J. Gulick, W.A. Ng, and J. Robbins. 1996. Ablation of the murine α-myosin heavy chain gene leads to dosage effects and functional deficits in the heart. *J. Clin. Invest.* 8:1906–1917.

21. McAuliffe, J.J., L.Z. Gao, and R.J. Solaro. 1990. Changes in myofibrillar activation and troponin C Ca^{2+} binding associated with troponin T isoform switching in developing rabbit heart. *Circ. Res.* 66:1204–1216.

22. Fewell, J.G., H. Osinska, R. Klevitsky, W. Ng, G. Sfyris, F. Bahreh-

mand, and J. Robbins. 1997. A treadmill exercise regimen for identifying cardiovascular phenotypes in transgenic mice. *Am. J. Physiol*. 273(3 Pt. 2):H1595–H1605.

23. Nguyen, T.T., E. Hayes, L.A. Mulieri, B.J. Leavitt, H.E. ter Keurs, N.R. Alpert, and D.M. Warshaw. 1996. Maximal actomyosin ATPase activity and in vitro myosin motility are unaltered in human mitral regurgitation heart failure. *Circ. Res.* 79:222–226.

24. Mulieri, L.A., G. Hasenfuss, F. Ittleman, E.M. Blanchard, and N.R. Alpert. 1989. Protection of human left ventricular myocardium from cutting injury with 2,3-butanedione monoxime. *Circ. Res.* 65:1441–1449.

25. Edman, K.A.P. 1979. The velocity of unloaded shortening and its relation to sarcomere length and isometric force in vertebrate muscle fibers. *J. Physiol*. 291:143–159.

26. Moss, R. 1986. Effects on shortening velocity of rabbit skeletal muscle due to variations in the level of thin-filament activation. *J. Physiol.* 377:487–505.

27. Ng, W.A., I.L. Grupp, A. Subramaniam, and J. Robbins. 1991. Cardiac myosin heavy chain mRNA expression and myocardial function in the mouse heart. *Circ. Res.* 68:1742–1750.

28. Barton, P.J., B. Robert, A. Cohen, I. Garner, D. Sassoon, A. Weydert, and M.E. Buckingham. 1988. Structure and sequence of the myosin alkali light chain gene expressed in adult cardiac atria and fetal striated muscle. *J. Biol. Chem*. 263:12669–12676.

29. Azizi, C., P. Bouiossou, F. Galen, A. Lattion, M. Lartigue, and A. Carayon. 1995. Alterations in atrial natriuretic peptide gene expression during endurance training in rats. *Eur. J. Endocrinol*. 133:361–365.

30. Izumo, S. 1988. Protooncogene induction and reprogramming of cardiac gene expression produced by pressure overload. *Proc. Natl. Acad. Sci. USA.* 85: 339–343.

31. Izumo, S., A.M. Lompre, R. Matsuoka, G. Koren, K. Schwartz, G.B. Nadal, and V. Mahdavi. 1987. Myosin heavy chain messenger RNA and protein isoform transitions during cardiac hypertrophy. Interaction between hemodynamic and thyroid hormone-induced signals. *J. Clin. Invest.* 79:970–977.

32. Schwartz, K., D. de la Bastie, P. Bouveret, P. Oliviero, S. Alonso, and M. Buckingham. 1986. α-Skeletal muscle actin mRNA accumulates in hypertrophied adult rat hearts. *Circ. Res.* 59:551–555.

33. Trahair, T., T. Yeoh, T. Cartmill, A. Keogh, P. Spratt, V. Chang, C.G. dos Remedios, and P. Gunning. 1993. Myosin light chain gene expression associated with disease states of the human heart. *J. Mol. Cell. Cardiol.* 25:577–585.

34. Sweeney, H.L. 1995. Function of the N terminus of the myosin light chain of vertebrate striated muscle. *Biophys. J*. 68(Suppl.):112–119.

35. Lowey, S., G.S. Waller, and K.M. Trybus. 1993. Function of skeletal muscle myosin heavy and light chain isoforms by an in vitro motility assay. *J. Biol. Chem*. 268:20414–20418.

36. Morano, I., O. Ritter, A. Bonz, T. Timek, C.F. Vahl, and G. Michel. 1995. Myosin light chain-actin interaction regulates cardiac contractility. *Circ. Res.* 76:720–725.

37. Whittaker, M., E.M. Wilson-Kubalek, J.E. Smith, L. Faust, R.A. Milligan, and H.L. Sweeney. 1995. A 35-Å movement of smooth muscle myosin and ADP release. *Nature*. 378:748–751.

38. Morano, I., K. Hädicke, H. Hasse, M. Böhm, E. Erdmann, and M.C. Schaub. 1997. Changes in essential myosin light chain isoform expression provide a molecular basis for isometric force regulation in the failing human heart. *J. Mol. Cell. Cardiol.* 29:1177–1187.

39. Lowes, B.D., W. Minobe, W.T. Abraham, M.N. Rizeq, T.J. Bohlmeyer, R.A. Quaife, R.L. Roden, D.L. Dutcher, A.D. Robertson, et al. 1997. Changes in gene expression in the intact human heart. Downregulation of alpha-myosin heavy chain in hypertrophied, failing ventricular myocardium. *J. Clin. Invest.* 100:2315–2324.

40. Nakao, K., W. Minobe, R. Roden, M.R. Bristow, and L.A. Leinwand. 1997. Myosin heavy chain gene expression in human heart failure. *J. Clin. Invest*. 100:2362–2370.

41. Colbert, M.C., D.G. Hall, T.R. Kimball, S.A. Witt, J.N. Lorenz, M.L. Kirby, T.E. Hewett, R. Klevitsky, and J. Robbins. 1997. Cardiac compartment-specific overexpression of a modified retinoic acid receptor produces dilated cardiomyopathy and congestive heart failure in transgenic mice. *J. Clin. Invest.* 100:1958–1968.

42. Sussman, M.A., S. Welch, N. Cambon, R. Klevitsky, T.E. Hewett, S.A. Witt, and T.R. Kimball. 1998. Myofibril degeneration caused by tropomodulin overexpression leads to dilated cardiomyopathy in juvenile mice. *J. Clin. Invest.* 101:51–61.